Proteomic Analysis of a Sea-Ice Diatom: Salinity Acclimation Provides New Insight into the Dimethylsulfoniopropionate Production Pathway[1][C][W][OA]

Barbara R. Lyon, Peter A. Lee, Jennifer M. Bennett, Giacomo R. DiTullio, and Michael G. Janech*

Hollings Marine Lab, Charleston, South Carolina 29412 (B.R.L., P.A.L., J.M.B., G.R.D.); Marine Biomedicine and Environmental Sciences Center, Medical University of South Carolina, Charleston, South Carolina 29412 (B.R.L.); Grice Marine Laboratory, College of Charleston, Charleston, South Carolina 29412 (P.A.L., J.M.B., G.R.D.); Division of Nephrology, Department of Medicine, Medical University of South Carolina, Charleston, South Carolina 29425 (M.G.J.); and Ralph H. Johnson Veterans Affairs Medical Center, Charleston, South Carolina 29425 (M.G.J.)

Dimethylsulfoniopropionate (DMSP) plays important roles in oceanic carbon and sulfur cycling and may significantly impact climate. It is a biomolecule synthesized from the methionine (Met) pathway and proposed to serve various physiological functions to aid in environmental stress adaptation through its compatible solute, cryoprotectant, and antioxidant properties. Yet, the enzymes and mechanisms regulating DMSP production are poorly understood. This study utilized a proteomics approach to investigate protein changes associated with salinity-induced DMSP increases in the model sea-ice diatom *Fragilariopsis cylindrus* (CCMP 1102). We hypothesized proteins associated with the Met-DMSP biosynthesis pathway would increase in relative abundance when challenged with elevated salinity. To test this hypothesis axenic log-phase cultures initially grown at a salinity of 35 were gradually shifted to a final salinity of 70 over a 24-h period. Intracellular DMSP was measured and two-dimensional gel electrophoresis was used to identify protein changes at 48 h after the shift. Intracellular DMSP increased by approximately 85% in the hypersaline cultures. One-third of the proteins increased under high salinity were associated with amino acid pathways. Three protein isoforms of *S*-adenosylhomo-cysteine hydrolase, which synthesizes a Met precursor, increased 1.8- to 2.1-fold, two isoforms of *S*-adenosyl Met synthetase increased 1.9- to 2.5-fold, and *S*-adenosyl Met methyltransferase increased by 2.8-fold, suggesting active methyl cycle proteins are recruited in the synthesis of DMSP. Proteins from the four enzyme classes of the proposed algal Met transaminase DMSP pathway were among the elevated proteins, supporting our hypothesis and providing candidate genes for future characterization studies.

Sea-ice diatoms are highly adaptive unicellular photosynthetic eukaryotes capable of forming dense microbial communities within sea-ice brine channels (Thomas and Dieckmann, 2002). To live within sea ice, organisms must acclimate to steep environmental gradients in temperature, salinity, light, and nutrients/gases encountered within the ice column (Fig. 1). Studies on psychrophilic diatoms have revealed some of the physiological mechanisms that enable them to survive these conditions. An increase in polyunsaturated fatty acids (PUFAs) is important for maintaining membrane fluidity at freezing temperatures (Morgan-Kiss et al., 2006). Furthermore, increases in PUFA composition within the thylakoid membrane enables increased electron flow under light limitation (Mock and Kroon, 2002b), compensates for pigment and protein loss under nitrogen limitation (Mock and Kroon, 2002a), and has been shown to confer salinity tolerance in the freshwater cyanobacterium, *Synechocystis* (Allakhverdiev et al., 1999). Polar diatoms also produce ice-binding proteins that serve as cryoprotectants via their ability to prevent ice recrystallization (Janech et al., 2006). Secretion of these proteins along with other exopolymeric substances likely serve to maintain brine channel structure (Krembs et al., 2002) and facilitate the retention of brine (Raymond et al., 2009; Krembs et al., 2011; Raymond, 2011). Exopolymeric substances, largely composed of glycoproteins, may also modify external microenvironments to minimize osmotic stress (Krembs and Deming, 2008). On the other hand, synthesis of amino acid osmolytes in response to salinity stress, such as Pro, help maintain internal osmotic balance in sea-ice diatoms (Krell et al., 2007). The compound dimethylsulfoniopropionate (DMSP) has also been found in high levels within sea-ice diatoms (Kirst et al., 1991; Levasseur, 1994;

[1] This work was supported by the National Science Foundation (grant nos. ANT–0739597 to M.G.J., ANT–0739446 to P.A.L. and G.R.D., and OPP0338097 to G.R.D.).

* Corresponding author; e-mail janechmg@musc.edu.

The author responsible for distribution of materials integral to the findings presented in this article in accordance with the policy described in the Instructions for Authors (www.plantphysiol.org) is: Michael G. Janech (janechmg@musc.edu).

[C] Some figures in this article are displayed in color online but in black and white in the print edition.

[W] The online version of this article contains Web-only data.

[OA] Open Access articles can be viewed online without a subscription.

www.plantphysiol.org/cgi/doi/10.1104/pp.111.185025

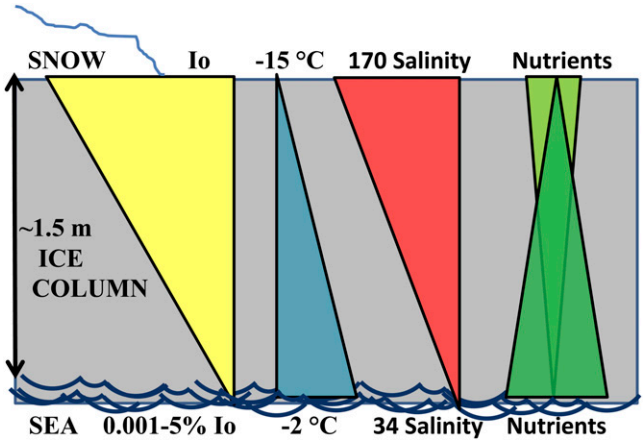

Figure 1. Sea-ice cross section illustrating strong gradients in abiotic variables. Incident surface irradiance (Io) is attenuated by snow cover and ice. Cold atmospheric temperatures freeze water and concentrate sea salts into high-salinity brine channels in which ice diatoms thrive. pH and alkalinity typically increase in part due to increasing concentrations of sea salts, although biological activity also strongly affects these parameters. Nutrients are replenished from the sea water below or flooding events over the top of the ice (adapted from Krell, 2006). [See online article for color version of this figure.]

DiTullio et al., 1998; Trevena et al., 2000; Lee et al., 2001), in stark contrast to the typically low levels seen in temperate diatoms (Keller et al., 1989). DMSP synthesis may be another physiological mechanism by which sea-ice diatoms combat environmental stress.

DMSP is the biogenic precursor to the climatically active sulfur compound, dimethylsulfide (DMS). Atmospheric oxidation of DMS to sulfate forms cloud condensation nuclei that can increase the Earth's albedo (reflective) effect (Charlson et al., 1987). Cloud condensation nuclei formation creates an interesting feedback loop between algae and their environment since algal production of DMSP can both modulate and be modulated by climate. Yet despite a considerable amount of prior research on the effects of environmental variables on DMSP production, there is still debate over its exact physiological function(s). For instance, various studies have shown intracellular DMSP concentrations increase in response to high salinity (Vairavamurthy et al., 1985), low temperatures (Karsten et al., 1992), variations in light (Karsten et al., 1990; Hefu and Kirst, 1997; Slezak and Herndl, 2003), and nutrient limitation (Gröne and Kirst, 1992; Sunda et al., 2002, 2007) to name a few. Factors found to influence DMSP production, taken together with several chemical properties of this compound, support three major physiological roles that would aid acclimation of photoautotrophic organisms to sea-ice conditions (Fig. 1) and explain high DMSP levels found in field samples. First, DMSP is a zwitterion and can serve as a compatible solute to reduce ionic disruption of enzyme activity and maintain protein conformation when the solute is present at high concentrations (Vairavamurthy et al., 1985; Kirst, 1990). Fluctuation of DMSP with temperature support its role as a cryoprotectant via its ability to reduce the loss of enzyme activity caused by low temperatures in the absence of DMSP (Nishiguchi and Somero, 1992). Furthermore, DMSP and several of its downstream metabolites are hydroxyl radical scavengers, and together form a powerful antioxidant cascade equivalent in reducing power to glutathione (Sunda et al., 2002).

The synthesis and regulatory pathways of DMSP are poorly understood. Met is the amino acid precursor for DMSP, but studies on higher plants and algae have revealed divergent pathways (Stefels, 2000). Higher plants use *S*-methyl-Met as an intermediate. Microalgae, such as sea-ice diatoms, are believed to utilize an alternative Met transaminase pathway. Radiolabeling studies of pathway metabolites showed algal DMSP synthesis sequentially utilizes 2-oxoglutarate-dependent aminotransferase, NADPH-linked reductase, *S*-adenosyl Met (SAM)-dependent methyltransferase (SAMmt), and oxidative decarboxylase (Gage et al., 1997; Summers et al., 1998). Analyzed most extensively in the green macroalgae, *Ulva intestinalis*, radiolabeled metabolites also supports presence of this pathway in haptophyte, diatom, and prasinophyte species. Interestingly, an alternative pathway has been proposed for dinoflagellates, starting with a Met decarboxylase, and presumably followed by aminotransferase and then methyltransferase steps (Kitaguchi et al., 1999). Yet, to our knowledge, the specific genes controlling DMSP production have yet to be identified in any DMSP-producing organism.

Previous experiments with *Fragilariopsis cylindrus* (CCMP 1102) have determined that salinity was the dominant abiotic stress on sea-ice diatoms (Krell, 2006). The deleterious effects of high salinity on photoautotrophs have been well established. For example, hypersaline conditions impart osmotic and ionic stress on cells. This stress leads to photosynthetic disruption, increased respiration, and growth arrest (Sudhir and Murthy, 2004). Salinity also causes indirect damage as a result of oxidative stress (Rijstenbil, 2005). Halotolerant red algae adjust their internal osmotic potential predominantly through the accumulation of K^+ and Cl^- ions and active export of Na^+ ions; organic osmolytes also accumulate but with lesser contributions to internal osmotic pressure (Mostaert et al., 1995). Compartmentalization of ions in the vacuole has been suggested to minimize ionic inhibition of cytoplasmic enzyme activity (Mostaert et al., 1996). Subcellular compartmentalization of organic osmolytes to the cytoplasm or other organelles would increase their local osmotic contribution, as was first suggested for mannitol in marine brown algae (Davison and Reed, 1985). Some organic osmolytes have also been proposed to serve dual roles as compatible solutes and antioxidants (Rodriguez and Redman, 2005). *F. cylindrus* organic osmolytes include Pro, Gly betaine, DMSP, and homarine (Krell, 2006). This proteomics investigation of *F. cylindrus* salinity-induced DMSP accumu-

lation was undertaken to identify proteins that are elevated when DMSP levels increase, as well as explore other salinity-tolerance protein changes that enable sea-ice diatoms to readily acclimate to hypersaline conditions. In an attempt to be more representative of natural salinity change, salinity was gradually manipulated over a 22-h period, and both pH and carbonate alkalinity were allowed to covary with salinity, as occurs within sea ice (Papadimitriou et al., 2007). We hypothesized that proteins associated with Met synthesis and from enzyme classes that drive reactions described in DMSP metabolite radiolabeling studies (Gage et al., 1997; Summers et al., 1998) will increase in abundance during hypersaline-induced DMSP accumulation. Identification of candidate proteins that may regulate DMSP synthesis will enable targeted studies on biological controls of DMSP production, which in turn can lead to improved modeling of environmental and biological feedbacks on potential DMS climate effects.

RESULTS

Hypersalinity Effects on DMSP, Growth, and Photosynthetic Efficiency of PSII

To mimic salinity changes encountered by polar diatoms during sea-ice formation, *F. cylindrus* cultures were gradually shifted from seawater with a salinity of 35 (total sea salts approximately 0.6 M) to a salinity of 70 (total sea salts approximately 1.2 M) over a 22-h period. This increase in salinity resulted in a concomitant doubling of media osmolality (Supplemental Table S1). The shift to high salinity initially depressed growth and photosynthetic efficiency of PSII (F_v/F_m), but cultures recovered to control levels by days 5 to 7 (Fig. 2, A and C). As hypothesized, intracellular particulate DMSP ($DMSP_p$) increased under salt stress. An 80% increase in the molar $DMSP_p$ concentration occurred quickly following the shift to high-salinity media and was sustained throughout the experiment (Fig. 2E). Similar results were found in a follow-up experiment scaled up to harvest biomass for a proteomics-based comparison of day 2 (T2) proteins (Fig. 2, B, D, and F).

Proteomic Response of *F. cylindrus* to Hypersalinity

Two-dimensional gel electrophoresis (2DE) was performed on five independent biological replicates per group using proteins isolated from T2 cell pellets (i.e. 48 h following start of salinity shift, 26 h after completion of dilution/salinity shift). Protein spots (n = 966) were matched across all gels (Fig. 3). Comparison of log-transformed, normalized spot intensities identified 80 distinct spots significantly changing ($\alpha \leq 0.02$) in relative abundance (Supplemental Table S2). This α-level setting was selected to minimize false

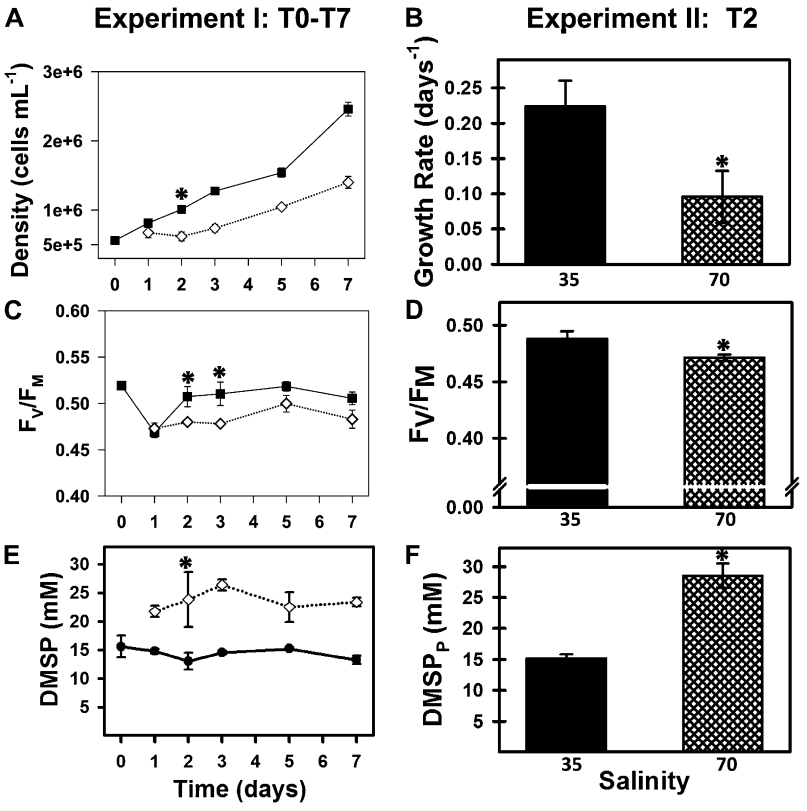

Figure 2. Left column (experiment I) shows growth, photosynthetic efficiency (F_v/F_m), and intracellular DMSP ($DMSP_p$) measured across 7 d (T0–T7) of an initial salinity stress experiment (three biological replicates per group). Right column (experiment II) shows day 2 (T2) values in follow-up experiment conducted for proteomics analysis at this time point (five biological replicates per group). Black squares, 35 control salinity; white diamonds, 70 treatment salinity; means and SES are graphed with asterisks indicating significant differences by Tukey's post-hoc. A, High-salinity shift decreased growth rate between days 0 and 3 ($P < 0.005$), after which growth rates were not significantly different from controls. B, Specific growth rate over first 2 d of salinity stress decreased 60% in experiment II ($P < 0.001$). C, F_v/F_m in experiment I is decreased under high salinity on T2 and T3 ($P < 0.01$), but not at later time points. D, In experiment II, F_v/F_m showed similar suppression (4%) in high salinity ($P < 0.02$). E, $DMSP_p$ significantly increased by 82% following salinity shift ($P < 0.01$) and remained elevated throughout experiment I. F, $DMSP_p$ was increased 87% under hypersalinity ($P < 0.00001$) at T2 in experiment II.

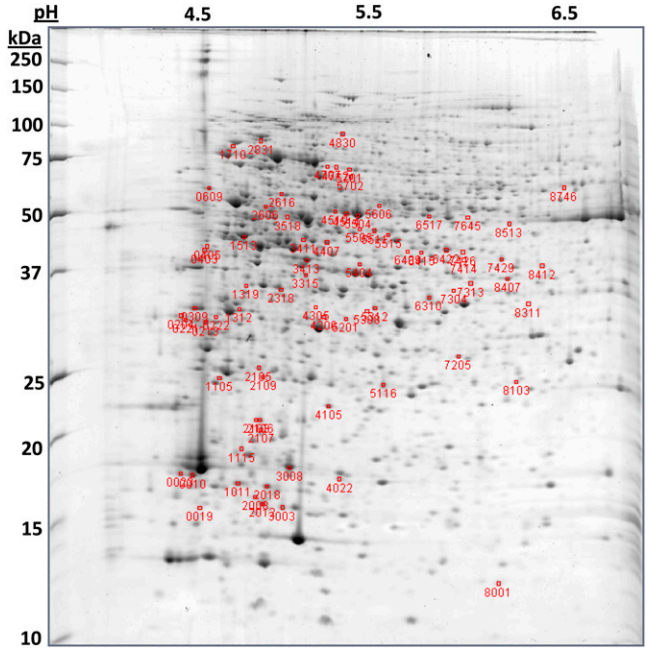

Figure 3. Representative 2D gel. Protein spots significantly changing in relative abundance in response to salinity are indicated by their gel spot number. MW markers are identified along the left axis and pH units along the top axis. [See online article for color version of this figure.]

discovery rate (FDR) without greatly affecting type II error. The FDR *q* value (reported in Supplemental Table S2) further assesses statistical confidence in observed relative abundance changes. Forty nine of the significantly changing spots increased in the hypersaline high DMSP condition compared to 31 spots that decreased in relative abundance under hypersalinity.

Sixty one significantly changing protein spots were selected for identification by tandem mass spectrometry (MS/MS). Spots were not selected if their relative intensity was deemed too low for identification or located within a smear on the gel. Scaffold analysis of 54 matrix-assisted laser desorption/ionization tandem time-of-flight (MALDI-TOF-TOF) samples searched against the *F. cylindrus* filtered database (using MASCOT and X! Tandem search algorithms) identified 39 of these proteins with a 1.9% protein FDR using 84 spectra identified at a 0.9% peptide FDR. To expand identifications, 19 protein spots were selected for liquid chromatography electrospray ionization MS/MS linear triple quad (LTQ) analysis (10 not identified via MALDI-TOF-TOF, seven not analyzed initially by MALDI-TOF-TOF, and two identified by MALDI-TOF-TOF to cross validate). Proteins were identified in all samples. In total, scaffold analysis of LTQ spectra (using SEQUEST and X! Tandem search algorithms) identified 110 proteins from 1,131 spectra at a 0.1% FDR. Because LTQ samples were separated out along a 60-min gradient, less-abundant proteins that comigrate in 2D gels were also identified. However, using spectrum counts, molecular weight (MW), and pI information, the protein spots were assigned to a single best hit protein (Supplemental Table S3), except for a few cases where a protein mix indicated two best hits. Complete LTQ-SEQUEST data from which best matches were selected is presented in an Excel workbook in Supplemental Table S4. A total of 36 of the high-salinity/DMSP elevated proteins and 16 of the decreased protein spots were identified.

Protein Changes of Hypersalinity Acclimation

Protein identifications for significantly changing protein spots are listed in Table I, along with relative fold-change, and eukaryotic orthologous group (KOG) enzyme classes. KOG salinity response classes include amino acid, carbohydrate, and coenzyme transport and metabolism, secondary metabolites biosynthesis, transport and catabolism, energy production and conversion, signal transduction mechanisms, posttranslational modification, protein turnover, chaperones, and defense mechanisms. Twelve of the 36 proteins that increased in relative abundance in the 70 salinity group are involved in amino acid synthesis and metabolism. Among this dataset were Orn aminotransferase isoforms and several other enzymes involved in the biosynthesis pathway of the amino acid osmolyte Pro. Another highly represented KOG class was coenzyme transport and metabolism; six of the proteins increased in high salinity/DMSP were annotated from this class. Proteins in this group include *S*-adenosyl homo-Cys hydrolase (SAHCyase), an enzyme in the synthesis pathway of the DMSP precursor Met and part of the SAM active methyl cycle. Three charge forms of this protein were elevated 1.8- to 2.1-fold in the high-salinity/DMSP group. Several other enzymes involved in the SAM methyl cycle were increased, including SAM synthetase (SAMsyn) charge forms elevated by 1.9- to 2.5-fold, and two putative SAMmt, one with multiple charge states, elevated by 2.3-, 2.8-, and 3.2-fold. The presence of different protein charge forms (i.e. different observed MW or pI) indicates posttranslational modifications or perhaps splice variants were present and changing in relative abundance in response to salinity.

2DE gels identified 18 *F. cylindrus* proteins within the four enzyme classes of the proposed algal DMSP transaminase synthesis pathway significantly increased in the high-salinity treatment. These enzyme classes are involved in a wide range of biological pathways, and while most could be assigned by homology as enzymes from well-characterized metabolic pathways, the function of five of these proteins were poorly characterized. Since they are elevated in association with increases in DMSP, we classified these as candidate genes for DMSP synthesis. These include an unknown aminotransferase (AT; SSP 1513), NADPH reductase (REDOX; SSP 7205), putative SAMmt (SSP 3518), and two putative decarboxylases, pyridoxyl-

Table I. *Hypersalinity response proteins in F. cylindrus*

2DE proteins spots (SSP) are listed from highest to lowest relative fold-change calculated as a ratio of normalized mean spot intensity in 70 compared to 35 salinity cultures. *P* values are reported for each spot, along with JGI protein accession number, name, and KOG information. Table abbreviations include: pr., Precursor; chlor, chloroplast; KOG groups include: M, metabolism; C, cellular processes and signaling; I, information storage and processing; P, poorly characterized; NA, no KOG homolog.

SSP	Fold Δ	*P* Value	Accession No.	Protein Name	KOG Group: Class
7426	4.79	0.000	277974	Acetylornithine aminotransferase	M: amino acid transport and metabolism
			270566	Pyrophosphate-dependent phosphofructo-1-kinase	M: carbohydrate transport and metabolism
5515	3.51	0.000	269005	Orn aminotransferase	M: amino acid transport and metabolism
4707	3.24	0.000	212856[a]	Putative sarcosine-dimethylglycine methyltransferase[b]	P: general function prediction only
6415	3.16	0.000	277974	Acetylornithine aminotransferase	M: amino acid transport and metabolism
			185436	Hypothetical protein	NA
1312	3.15	0.005	273578	Mitochondrial translation elongation factor EF-Tsmt	I: translation, ribosomal structure and biogenesis
5404	3.13	0.000	203522	Pyrroline-5-carboxylate reductase	M: amino acid transport and metabolism
5511	3.10	0.006	269005	Orn aminotransferase	M: amino acid transport and metabolism
5505	2.76	0.005	269005	Orn aminotransferase	M: amino acid transport and metabolism
3518	2.75	0.018	207357	Putative SAM-dependent carboxyl methyltransferase[b]	NA
204	2.70	0.003	261222	Collagens (type IV and type XIII), and related proteins	C: extracellular structures
2318	2.62	0.001	275170	N-acetyl-gamma-glutamyl-phosphate reductase	M: amino acid transport and metabolism
6517	2.51	0.000	271944	*S*-adenosylmethionine synthetase	M: coenzyme transport and metabolism
5701	2.41	0.007	177646	ALDH	M: energy production and conversion
3411	2.40	0.002	187807	Glutamate 1-semialdehyde 2,1-aminomutase	M: amino acid transport and metabolism
2616	2.37	0.001	238865	Putative pyridoxal-dependent decarboxylase[b]	NA
4712	2.30	0.000	212856[a]	Putative sarcosine-dimethylglycine methyltransferase[b]	P: general function prediction only
403	2.26	0.003	212738	Ser carboxypeptidase (lysosomal cathepsin A)	C: posttranslational modification, protein turnover
4514	2.13	0.010	170146	*S*-adenosylhomocysteine hydrolase	M: coenzyme transport and metabolism
4510	2.11	0.001	170146	*S*-adenosylhomocysteine hydrolase	M: coenzyme transport and metabolism
7645	1.88	0.000	271944	*S*-adenosylmethionine synthetase	M: coenzyme transport and metabolism
5504	1.76	0.004	170146	*S*-adenosylhomocysteine hydrolase	M: coenzyme transport and metabolism
2105	1.68	0.000	269315	ThiJ/PfpI family (putative transcriptional regulator DJ-1)	C: defense mechanisms; P: general function
2606	1.65	0.019	263016[a]	DiDECARB	M: amino acid transport and metabolism
4206	1.64	0.005	267582	Glutathione *S*-transferase	C: posttranslational modification, protein turnover
609	1.62	0.009	272749	Iron starvation induced protein (ISIP2A)[b]	NA
7429	1.58	0.005	268209	Alcohol dehydrogenase class V	M: secondary metabolites biosynthesis, transport
3413	1.55	0.004	270038	Fructose 1,6-bisphosphate aldolase	M: carbohydrate transport and metabolism
5201	1.51	0.010	267582	Glutathione *S*-transferase	C: posttranslational modification, protein turnover, chaperones
7205	1.50	0.003	173405	NADPH-dependent FMN reductase (predicted flavoprotein)	P: general function prediction only
3315	1.41	0.004	170890	Fructose- 1,6-bisphosphatase	M: carbohydrate transport and metabolism
4407	1.40	0.020	187808	Glu 1-semialdehyde 2,1-aminomutase	M: amino acid transport and metabolism
1513	1.37	0.017	273803	Unknown transaminase (kynurenine aminotransferase)	M: amino acid transport and metabolism
1011	1.31	0.000	269494	Cu2+/Zn2+ SOD1	M: inorganic ion transport and metabolism
6422	1.26	0.011	258994	Fructose 1,6-bisphosphate aldolase	M: carbohydrate transport and metabolism
5312	1.22	0.013	269867	Glyceraldehyde-3-phosphate dehydrogenase	M: carbohydrate transport and metabolism
			207931	Transaldolase	M: carbohydrate transport and metabolism
8407	1.19	0.002	268607	Pyridoxal (vitB6) biosynthesis lyase (stationary phase-induced protein)	M: coenzyme transport and metabolism
6310	−1.35	0.005	272954	Hypothetical protein	NA
213	−1.43	0.009	203554	DNA polymerase Δ processivity factor (PCNA)	I: replication, recombination, and repair
10	−1.45	0.019	272028	Fucoxanthin-chlorophyll a-c binding protein, chlor pr.	NA
23	−1.49	0.016	272028	Fucoxanthin-chlorophyll a-c binding protein, chlor pr.	NA

(*Table continues on following page.*)

Table I. (*Continued from previous page.*)

SSP	Fold Δ	*P* Value	Accession No.	Protein Name	KOG Group: Class
2018	−1.52	0.001	272228	Cytochrome b6-f complex iron-sulfur subunit, chlor	M: energy production and conversion
2012	−1.53	0.001	269837	ATP-dependent Clp protease adaptor protein ClpS	NA
			170761	Fucoxanthin-chlorophyll a-c binding protein C, chlor pr.	NA
3008	−1.54	0.011	273006	Fucoxanthin, chlorophyll protein1	NA
2106	−1.76	0.018	174589	Fucoxanthin chlorophyll a/c-binding protein pr.	NA
4105	−1.90	0.007	206118	PSII oxygen evolving complex protein	NA
5116	−1.92	0.004	172948	Chloroplast light harvesting protein isoform12	NA
221	−2.01	0.016	268130	FKBP-type peptidyl-prolyl cis-trans isomerase	C: posttranslational modification, protein turnover
3003	−2.04	0.007	170761	Fucoxanthin-chlorophyll a-c binding protein D, chlor pr.	NA
309	−2.31	0.015	261222	Collagens (type IV and type XIII), and related proteins	C: extracellular structures
1105	−2.62	0.002	243823	Hypothetical protein	NA
2008	−2.63	0.002	170761	Fucoxanthin-chlorophyll a-c binding protein C, chlor pr.	NA
2107	−2.68	0.011	174584	Fucoxanthin chlorophyll a/c-binding protein pr.	NA

[a]Protein accession from all models database. [b]Protein name manually annotated based on National Center for Biotechnology Information blastp search (see Supplemental Table S7).

dependent decarboxylase (DECARB; SSP 2616) and diaminopimelate decarboxylase (DiDECARB; SSP 2606), which were elevated by 1.4-, 1.5-, 2.8-, 2.4-, and 1.7-fold, respectively (see Supplemental Table S3).

Protein changes also shed insight into general salinity acclimation mechanisms. For instance, antioxidant proteins that increased under hypersalinity included superoxide dismutase (SOD), glutathione *S*-transferase (GST), and vitamin B_6 biosynthesis protein. Several carbohydrate metabolism proteins also increased in the high-salinity treatment. Interestingly, the vast majority of decreased proteins were fucoxanthin-chlorophyll binding proteins (FCPs), as well as other photosynthetic proteins. Proliferating nuclear cell antigen involved in cell division was also depressed in the hypersaline group.

RNA Changes during Hypersaline Acclimation

RNA abundance from several SAM methyl cycle and FCP proteins were compared using quantitative real-time PCR (qPCR). The 18s RNA housekeeping gene was used to normalize mRNA abundance of target genes. Transcript abundances for SAM methyl cycle enzymes SAHCyase, SAMsyn, and SAMmt were all significantly elevated at days 2 (T2) and 7 (T7) in the high-salinity/DMSP group (Fig. 4; Supplemental Table S5). Most notable was the 10- and 15-fold increase of SAMmt at T2 and T7, respectively ($P < 0.0001$). The FCP transcripts, however, followed an opposite pattern to that of the FCP protein abundance. Transcripts for the two FCP proteins quantified were elevated 1.5- and 2.1-fold at T2 ($P = 0.036$; $P = 0.005$, respectively) and 4.6- and 8-fold at T7 ($P = 0.020$; $P = 0.004$, respectively).

Protein Chloroplast-Targeting Presequences

Potential DMSP synthesis pathway proteins identified in protein gels were screened for chloroplast-targeting sequences using the programs SignalP and TargetP. Scores from these online tools are presented in Supplemental Table S6. Signal peptides were also manually screened for the most essential amino acids of the well-characterized diatom chloroplast localization motif, ASAFAP; the underlined amino acids have been experimentally determined to be the most integral for chloroplast import, although certain substitutions (G/S for A and W/Y/L for F) are also prevalent (Gruber et al., 2007). Chloroplast bipartite presequences are predicted for the AT, SAMmt, and DiDECARB (Fig. 5; Supplemental Table S6). Two of the five signalP scoring methods predict a bipartite signal peptide on an N-terminal splice variant of REDOX and there are potential chloroplast-targeting motifs within the presequence. The DECARB gene, however, is not predicted to have signal or transit peptides, although there is a possible chloroplast motif evident on the peptide presequence.

DISCUSSION

This study utilized gel-based proteomics to identify protein changes associated with hypersalinity-induced DMSP production in the sea-ice diatom *F. cylindrus*. Ice diatoms are halotolerant organisms found to contain relatively high DMSP concentrations, especially compared to pelagic diatoms (Levasseur, 1994). Hypersalinity conditions that typically occur within brine channels resulted in an approximately

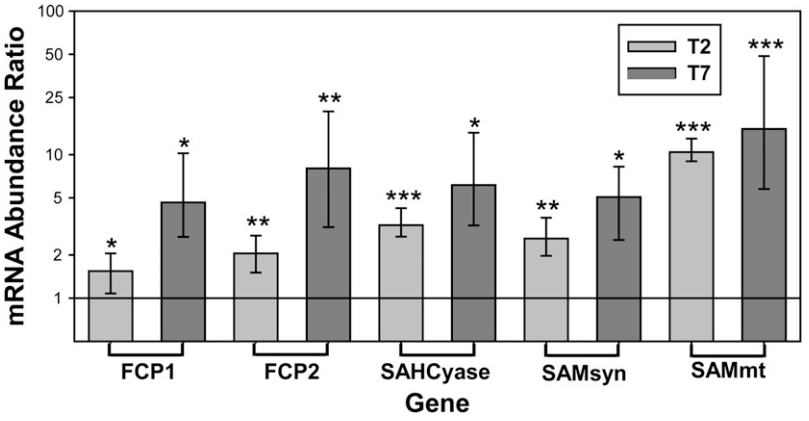

Figure 4. Relative mRNA abundance ratios at 70 salinity compared to 35 salinity are graphed in the log scale. The horizontal line at 1 demarcates no expression change was observed between treatment groups and values above that line indicates an increase in transcript abundance under high salinity. Transcripts for FCPs (FCP1 and FCP2), as well as the active methyl cycle genes SAHCyase, SAMsyn, and SAMmt increased in hypersaline conditions 2 (T2) and 7 (T7) d following start of 22-h salinity shift. Error bars show SES calculated with REST software. *$P < 0.05$, **$P < 0.01$, ***$P < 0.0001$.

85% increase in intracellular DMSP concentration relative to the 35 salinity treatment in two independent experiments. Unlike previous *F. cylindrus* salinity experiments where instantaneous shifts from salinities of 35 to 70 drastically reduced growth rate and F_v/F_m for several weeks (Krell, 2006), this study demonstrated the ability of *F. cylindrus* to rapidly acclimate to a gradual salinity shift (i.e. 35–70 salinity shift over a 22-h period). This gradual shift is more representative of natural salinity transitions during sea-ice formation and provides time for the induction of acclimatory mechanisms. $DMSP_p$ accumulation likely aids in the acclimation process due to its properties as a compatible solute and antioxidant. If DMSP is in fact scavenging hypersaline-induced hydroxyl radicals, in accordance with the DMSP antioxidant cascade proposed by Sunda and colleagues (2002), then $DMSP_p$ concentrations measured in these experiments are likely underestimates of DMSP production rates as a consequence of DMSP turnover to its metabolites DMS, dimethyl sulfoxide, and methane sulfinic acid. We are assuming that under nutrient-replete control conditions turnover is not elevated relative to cultures exposed to high salinity, a known condition to generate reactive oxygen species in diatoms (Rijstenbil, 2005). Quantification of DMSP synthesis enzymes could provide a surrogate method for qualitatively assessing $DMSP_p$ production; however, these enzymes must first be clearly identified and functionally characterized.

Candidate DMSP Synthesis Enzymes

We hypothesized Met-DMSP synthesis pathway enzymes would be elevated during hypersaline DMSP accumulation. Proteomics results supported the hypothesis and provided candidate genes for DMSP synthesis enzymes. For example, SAHCyase synthesizes homo-Cys, the precursor for Met. Three charge forms of this protein (different charge states separated on the gel) increased by 1.8- to 2.1-fold in association with elevated $DMSP_p$. SAHCyase transcripts were also elevated by 3.2- and 6.1-fold at T2 and T7, respectively. Met synthase (METsyn) converts homo-Cys to Met but was not among the elevated proteins identified. This absence could be due to the fact that *F. cylindrus* METsyns are approximately 100 kD and therefore located in the more poorly resolved high-MW gel region, making identification and quantification difficult using gel-based techniques. Results also supported the hypothesis that proteins from the enzyme classes proposed to be responsible for algal

	1 10 20 30 40 50 60 70
ATalt*	MKFTSSIVCAVAALSASSSTAFAFAPQGGRQSVSTAVFSTAADPAVSQVDRNENFAKLAGGYLFPEIGRR
REDOXalt	MPIKILYTFFAFASHRLTIIKSLYRNTIRIASSNTQTHTMSSKNVVLKTVVFMGSARDITPPWGGGSRLG
SAMmt*	MIGASFYAAATIIYCTSATFHTGAVTAFALKQQQQTVPTANSNVVHTPVGKDGDGAYSAATKGCFDVIDA
DECARB	MSFANNNDARMSFSTMPVQVFEEEPYESAKAKGFDDFEAMLTCGGDDRSLILESSTNKYHIRPQPVDPAH
DiDECARB*	MRLSFSTATIAAIAVTMLSSPSCNAFAPVQRHSGPSTSALSVSVSTDAPADTSVFLTAESAKACTDLAGS

Figure 5. Potential *F. cylindrus* DMSP pathway enzymes were screened for signal and transit peptides and variants of the diatom chloroplast-targeting motif ASAFAP. N-terminal variants are noted as alt for alternative splice variant. Asterisk (*) indicates significant probability of chloroplast-targeting presequence based on Target P and Signal P predictions. Bold letters, predicted signal peptide; gray highlight, predicted cleavage site motif; yellow highlight, manually predicted cleavage site based on motif characterization by Gruber et al. (2007); underlined, predicted transit peptide; red letters, conserved domain of mature protein.

conversion of Met to DMSP based on radiolabeling metabolite studies (Gage et al., 1997; Summers et al., 1998) would be elevated in association with salinity-induced DMSP elevation. Eighteen of the 36 proteins increased under high-salinity/DMSP conditions classified within the four enzyme classes in the proposed Met-DMSP synthesis pathway (Fig. 6). While a number of these could be assigned to other salinity-responsive enzymatic pathways based on various annotation databases (Supplemental Table S3), several do not have characterized substrates/pathways and therefore were assigned as candidate DMSP synthesis enzymes.

According to the proposed algal DMSP synthesis pathway (Gage et al., 1997; Fig. 6), the first step to convert Met to DMSP is catalyzed by an oxoglutarate-dependent AT, creating the intermediate metabolite 4-methylthio-2-oxobutyrate. In general, ATs were the most common proteins elevated under high-salinity/DMSP conditions. Four different genes can account for the eight AT isoforms found by 2DE. While KOG, gene ontology, and conserved domain annotations assign most proteins to roles in Pro and tetrapyrrole biosynthesis, one is classified as an unknown AT (Fc273803). This AT was elevated by 1.4-fold and most closely resembled a kynurenine AT whose substrate is oxoglutarate. The second step in the proposed pathway is NADPH-dependent reduction of 4-methylthio-2-oxobutyrate to 4-methylthio-2-hydroxybutyrate. There were a total of five NADPH-dependent reductases elevated under high salinity. Two of these reductases are enzymes involved in the synthesis of the osmolyte Pro, two are putative aldehyde dehydrogenases (ALDHs), while the fifth is annotated as a poorly characterized NADPH-dependent flavinoid reductase (Fc173405). The penultimate step in the DMSP transaminase pathway converts 4-methylthio-2-hydroxybutyrate to 4-dimethylsulfonio-2-hydroxybutyrate by a SAMmt. This enzyme has been shown to be an important control point in the synthesis of DMSP (Ito et al., 2011). Three elevated protein spots were identified as SAMmt. Two of the elevated SAMmt protein spots were different charge forms of Fc212856, a putative SAMmt with similarity to sarcosine dimethyl-Gly methyltransferase. Sarcosine dimethyl-Gly methyltransferase is an alternate synthesis pathway for the osmolyte Gly betaine that does not produce hydrogen peroxide as a by-product like the traditional choline oxidase pathway (Waditee et al., 2005). Substrates for the third SAMmt protein spot (Fc207357, relative protein abundance elevated 2.8-fold and transcripts elevated 10- to 15-fold in high-salinity/DMSP conditions) have not been characterized. It has similarity to higher-plant small molecule methyltransferases, containing all three of the required SAM-binding domains identified through crystal structures of salicylic acid and caffeine methyltransferases (Zubieta et al., 2003; McCarthy and McCarthy, 2007) but shows considerable divergence in substrate-binding regions. The last step in DMSP synthesis is the oxidative decarboxylation of 4-dimethylsulfonio-2-hydroxybutyrate to form DMSP. There were two putative pyridoxal-dependent decarboxylases (Fc238865 and Fc263016) that were elevated by 2.4- and 1.7-fold, respectively. Specific substrates are not apparent for either based on homology. Although direct evidence for the involvement of

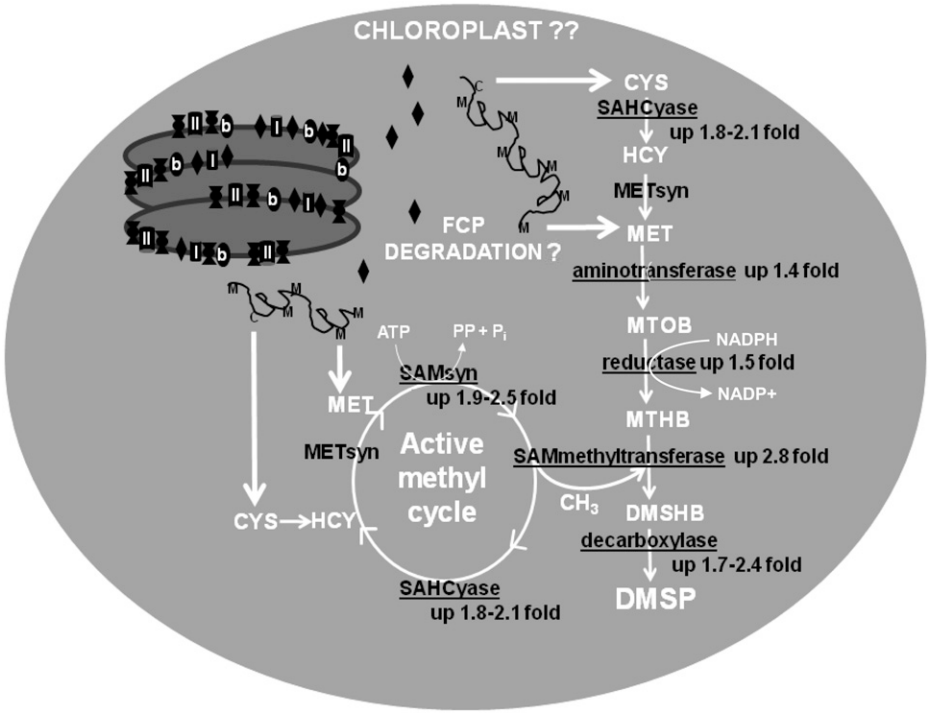

Figure 6. Proteins identified in this study represent the four enzyme classes of the proposed algal Met-DMSP synthesis pathway (adapted from Gage et al., 1997; Summers et al., 1998) and active methyl cycle proteins that are important for regenerating the SAM methyl donor for the penultimate step in DMSP synthesis. Underlined proteins increased with hypersalinity-induced DMSP accumulation. Based on lack of de novo Met synthesis proteins, presence of chloroplast-targeting preseqences on potential DMSP pathway enzymes, coupled with decreases in FCPs, we propose FCPs provide MET/CYS precursors for chloroplast-localized DMSP synthesis to help protect photosynthetic machinery from osmotic and oxidative damage.

these proteins in DMSP production is not presented, based on correlations in abundance with $DMSP_p$ and the correlation with proposed enzyme classes required for the metabolism of Met to DMSP, it is intriguing to speculate that the proteins identified using a proteomic approach may indeed be key enzymes necessary for the production of DMSP in sea-ice algae.

Homologs for AT (Fc273803), REDOX (Fc173405), SAMmt (Fc207357), and DiDECARB (Fc263016) were found in both the low DMSP-producing diatom *Thalassiosira pseudonana* (http://genome.jgi-psf.org/Thaps3/Thaps3.home.html) and the globally significant, high DMSP-producing haptophyte, *Emiliania huxleyi* (http://genome.jgi-psf.org/Emihu1/Emihu1.home.html). Interestingly, *E. huxleyi* shows three different proteins with similarity to SAMmt and also a homolog to DECARB (Fc238865), perhaps providing genetic explanation for their high DMSP production. On the other hand, some strains of the temperate diatom *Phaeodactylum tricornutum* do not have any detectable levels of DMSP (Keller et al., 1989). The *P. tricornutum* genome (http://genome.jgi-psf.org/Phatr2/Phatr2.home.html) has homologs to AT, REDOX, and DiDECARB, but not SAMmt or DECARB, possibly explaining an inability to synthesize DMSP.

The importance of the SAM active methyl cycle to compatible solute/DMSP production is reflected by the increased abundance of several SAMsyn (1.9- to 2.5-fold) and SAHCyase (1.8- to 2.1-fold) proteins produced under hypersalinity conditions (Table I). In addition to proteomic evidence, qPCR data also revealed elevated RNA levels of these genes by 2.6- to 5.1-fold and 3.2- to 6.1-fold, respectively (Fig. 4). The only active methyl cycle enzyme not identified in the hypersalinity dataset was METsyn whose gel resolution was limited by its large size. Previous studies have also documented salinity-induced increases in SAMsyn genes (Krell et al., 2007; Pulla et al., 2009). SAMsyn is responsible for the regeneration of SAM, the required cofactor for the penultimate methyltransferase reaction in DMSP synthesis. Active methyl cycle genes are also involved in the synthesis of other osmolytes such as pinitol, a sugar alcohol produced by succulent plants (Vernon and Bohnert, 1992), as well as in the methyltransferase synthesis pathway for Gly betaine (Nyyssölä et al., 2001) that also appears to be utilized by *F. cylindrus*.

Amino Acid Metabolic Changes Important for Osmolyte Synthesis

Acclimation to hypersaline environments necessitates that cells restore their intracellular osmotic/ionic balance to maintain viable enzymatic activity. Amino acid biosynthesis pathways feed directly into the synthesis pathways of the three main compatible solutes Pro, Gly betaine, and DMSP present in *F. cylindrus* (Krell, 2006). It is therefore not surprising that this is the dominant class of hypersalinity response proteins in *F. cylindrus* (Table I). Pro has been cited as the most abundant osmolyte in *F. cylindrus* (Krell et al., 2007) and proteomic results confirm Pro synthesis enzymes increased under hypersaline conditions. Pro is synthesized through the Arg/Orn/urea pathway (Cybis and Davis, 1975). *N*-acetyl γ-glutamyl phosphate reductase, acetyl-Orn aminotransferase, Orn aminotransferase, and pyrroline-5-carboxylate reductase are all involved in Pro synthesis and accounted for seven of the 36 proteins identified in the 70 salinity treatment group.

Metabolic Shifts to Meet Amino Acid Synthesis Energy Demands

Important to salinity acclimation is a prioritization of essential cell metabolic processes. Osmolyte and compatible solute synthesis is energetically demanding, yet essential to the maintenance of cellular homeostasis. Therefore, to meet these increased energy demands, enzymes from glycolysis and other carbohydrate metabolic pathways increase in relative abundance (Table I). These changes are likely coordinated by the 3.2-fold increase in mitochondrial translation elongation factor that initiates GTP-driven association of tRNAs to ribosomes for synthesis of mitochondrial genes (Beligni et al., 2004). This increase was accompanied by hypersaline-induced increases in the glycolytic enzymes Fru 1,6-bisphosphate aldolase, glyceraldehydes-3-P dehydrogenase, and pyrophosphate-dependent phosphofructo-1-kinase. Because the latter two proteins were identified in mixed protein spots (with another protein contributing a large portion of the spectrum counts), these data must be interpreted cautiously given the methodological limitations. However, utilization of pyrophosphate-dependent phosphofructo-1-kinase is an intriguing acclimation mechanism to replace the more typical ATP-dependent form, thereby conserving ATP for other metabolic processes (Ronimus and Morgan, 2001). Glyceraldehyde-3-P dehydrogenase is interesting because it is key to generating the energetic cofactor NADPH (Gao and Loescher, 2000) utilized by several of the other enzymes elevated in response to hypersalinity, including the second step in DMSP synthesis. Other elevated metabolic enzymes included alcohol dehydrogenase (part of anaerobic metabolism), as well as Fru 1,6-bisphosphatase and possibly transaldolase (another mixed protein spot), both involved in carbon skeleton rearrangements and conversions between alternate metabolic pathways.

General Stress Response Proteins

Oxidative stress is a well-documented indirect effect of salinity stress. Hence, it is not surprising to find that antioxidant proteins were elevated in the 70 salinity treatment group. Increased relative abundance of SOD adds further support for its involvement in alleviating salinity-induced oxidative stress. SOD increases have previously been reported in several other salinity

studies (Krell, 2006; Koca et al., 2007; Srivastava et al., 2008; Pandhal et al., 2009). Furthermore, SOD activity and corresponding antioxidants are known to be elevated in diatoms subjected to both high-salinity and high-light conditions (Janknegt et al., 2008). GST also helps protect cells against oxidative damage by conjugating hydroperoxides to form glutathione disulfides (Edwards et al., 2000) thus reducing salt-stress-induced lipid peroxidation (Katsuhara et al., 2005). It has also been proposed to protect proteins from irreversible oxidative damage and serve in oxidative stress signal transduction mechanism via protein glutathiolation of electrophilic/hydrophobic amino acid residues (Klatt and Lamas, 2000). Two charge states of GST in the hypersalinity treatment were elevated by 1.5- and 1.6-fold relative to the control treatment. Vitamin B_6 biosynthesis protein (also known as pyridoxal biosynthesis lyase or stationary phase-induced protein) was elevated by high salinity. This enzyme synthesizes pyridoxine, the precursor for pyridoxal-5-P, an important cofactor for many enzymatic reactions including ATs and DECARBs (see enzyme class cofactors, Supplemental Table S3). Vitamin B_6 has also been shown to have antioxidant activity (Mahfouz and Kummerow, 2004). ALDH, elevated 2.4-fold in high salinity and classified under energy production and conversion, could also be considered an antioxidant. Chemically reactive aldehydes can accumulate when environmental stress perturbs metabolic balance and, in turn, damage cells, but ALDHs protect against this (Sunkar et al., 2003). Several salinity-inducible ALDH protein families have been documented in Arabidopsis (*Arabidopsis thaliana*), including one whose overexpression decreases peroxidated lipid aldehydes (Kirch et al., 2004). Such an enzyme would be valuable in an organism like *F. cylindrus* where PUFAs are important for membrane stability. Alternatively, another form of ALDH is involved in the choline oxidase Gly betaine synthesis pathway (Kumar et al., 2004) consistent with hypersaline production of betaine. Lastly, iron starvation-induced protein (ISIP2A, Fc 272749) was elevated by 1.6-fold. Studies in the temperate diatom *P. tricornutum* found this gene transcript to be highly increased under iron starvation (Allen et al., 2008). Genomic annotation in the multicellular brown algae *Ectocarpus siliculosus* (Cock et al., 2010) identified a Fc272749 homolog as a probable high-CO_2 inducible periplasmic protein (Supplemental Table S5). The increase of ISIP2A in response to increased salinity points to the possibility that this protein may be an important general stress response protein, although its exact function is still unclear.

Chaperones and proteases are general stress response proteins that in our study show bidirectional changes under hypersaline conditions. A ThiJ/PfpI family protein contains a domain similar to the heat shock protein HSP31 from *Escherichia coli* that has chaperone and protease activity and is responsive to environmental stress (Wilson et al., 2004). This protein increased in abundance 1.7-fold at 70 salinity. Another protease, Ser carboxypeptidase, increased 2.3-fold. This large family of protein-hydrolyzing enzymes performs diverse functions involved in protein turnover, processing, and stress response (Feng and Xue, 2006). Interestingly, two other chaperone/protease-associated proteins, ATP-dependent Clp protease adaptor protein (ClpS), and FKBP-type peptidyl-prolyl cis-trans isomerase, decreased in high salinity. Although ClpS resided in a mixed protein spot and as such abundance changes were not conclusive, it is interesting to note that the Clp complex mediates protease activity in the chloroplast and this adaptor protein has been found to inhibit ClpAP substrate affinity (Dougan et al., 2002). Hence a decrease in this adaptor protein lends support to potential FCP-targeted protease activity being elevated in these cells. Peptidyl-prolyl isomerases act on protein imide bonds and are believed to coordinate protein folding, signal transduction, trafficking, assembly, and cell cycle regulation (Göthel and Marahiel, 1999). Interestingly, a member of this family has been shown to specifically modulate PSII complex formation (Lima et al., 2006) and the hypersalinity observed decrease could be associated with PSII FCP assembly changes.

Chloroplast Protein Changes

Salinity stress typically produces drastic impairments on various photosynthetic parameters, particularly in F_v/F_m. Such a reduction in photosynthetic competency, however, was not the case for *F. cylindrus* despite a doubling in salinity. Although F_v/F_m was reduced, this decrease was relatively minor. A striking feature of the protein dataset, however, was that 11 of the 16 proteins that were depressed were PS-related proteins. Cytochrome b_6f was reduced 1.5-fold and PSII oxygen-evolving complex protein decreased by 1.9-fold relative to the control. The latter protein has been found to be important in stabilization of the PSII complex (Yi et al., 2007). Interestingly, the other nine protein spots belonged to the FCP multigene family of light-harvesting antennae complexes (Lhc) that absorb and transfer photon energy to PS reaction centers and can also aid in the dissipation of excess energy. All of the FCPs identified belong to the most common FCP clade, Lhc-f, which is believed to be involved in binding of traditional light-harvesting pigments, as opposed to the Lhc-x clade believed to bind xanthophyll cycle pigments and aid in environmental stress acclimation (B.R. Green, personal communication). The limited suppression of F_v/F_m despite the decrease in FCPs could simply be due to a change in FCP organization. For instance, recent work using Resonance Raman spectroscopy has shown FCPs to be a modular flexible system where shifts in oligomerization and subunit composition can alter pigment binding and energy transfer (Premvardhan et al., 2009). Interestingly, two FCP transcripts examined by qPCR (Fc170761 and Fc174589), showed an elevation of 1.5- and 2-fold at T2. The elevation in transcript abundance

may indicate an initial effort to replace FCP proteins that are degraded as an initial response to high salinity. Such a discrepancy between mRNA and protein abundance is not uncommon (Greenbaum et al., 2003) and may provide insight into the complex nature of FCP regulation.

There are several possibilities for the observed decrease in FCPs. FCPs could be relatively more sensitive to salinity degradation compared to other proteins. Another explanation could be that a common stress response regulatory node responds to high salinity and light stress, decreasing FCPs to avoid oxidative stress via excess excitation from increased electron flow. A third explanation for degradation of a subset of FCPs is that it provides a chloroplast pool of amino acids (i.e. Cys and Met) for synthesis of DMSP and other stress response molecules. Compatible solutes are integral to preventing hypersalinity-induced damage and disruption of the photosynthetic apparatus. The zwitterionic nature of these compounds makes passive diffusion across the chloroplast membranes difficult. Trossat and colleagues (1998) showed that DMSP and its synthesis precursor in higher plants, *S*-methyl-Met, was localized within the chloroplast (and doubled in response to salinity). AT, SAMmt, and DiDECARB candidate DMSP synthesis genes all show clear chloroplast-targeting motifs (Fig. 5). Although there is weak evidence for a chloroplast presequence on the REDOX gene and no signal/transit peptide predicted for the DECARB, diatom studies have established that while this motif predicts chloroplast localization, it is not always present in chloroplast proteins (Gruber et al., 2007). Previous work by Gröne and Kirst (1992) found DMSP synthesis to be inhibited by addition of protease inhibitors, indicating that protein turnover was a source for DMSP precursors. FCPs are the most abundant transcripts in EST libraries (Scala et al., 2002; Mock et al., 2005). Furthermore, incubations with $H^{14}CO_3^-$ followed by autoradiography of membrane proteins separated by denaturing PAGE found protein bands corresponding to the 17.5- and 18.5-kD bands detected by FCP antibody account for 6% of membrane protein synthesis under high-light versus 18% under low-light conditions (Friedman and Alberte, 1986). Hence, FCPs represent a relatively large dynamic protein pool. In *F. cylindrus*, FCPs contain an average of eight Met and one Cys moieties per molecule that could serve as DMSP precursors. Given the decrease in FCPs without appreciable declines in F_v/F_m, in conjunction with the increase in proteases, lack of de novo Met synthesis enzymes (via the sulfate assimilatory pathway) among the increased proteins, and presence of chloroplast motifs on three of the four candidate DMSP synthesis enzymes, it is proposed that FCP turnover from this highly abundant chloroplast protein pool might provide the DMSP pathway with amino acid precursors within the chloroplast (Fig. 6). In turn, elevated DMSP production provides osmotic and oxidative protection of the photosynthetic apparatus.

CONCLUSION

This study demonstrated that DMSP accumulation was one of many physiological acclimation mechanisms utilized by the sea-ice diatom *F. cylindrus* in response to salinity stress. In addition, the study implicated several candidate DMSP synthesis genes that belong to enzyme classes of the proposed algal DMSP transaminase synthesis pathway. The large number of SAM active methyl cycle proteins elevated in the high-salinity/DMSP condition point to the importance of this cycle for DMSP synthesis. Proteomic results suggested the synthesis of multiple osmolytes and antioxidants, along with FCP degradation, were important cellular responses during salinity acclimation. Further studies utilizing transgenic methods to characterize the contribution of individual candidate DMSP synthesis genes will help to assemble this elusive cellular pathway. Understanding the impact of environmental parameters on the cellular responses associated with DMSP production will improve numerical DMS models to predict and understand the effects of climate change and sea-ice loss on global biogeochemical cycles.

MATERIALS AND METHODS

Culture Conditions

Axenic, semicontinuous cultures of *Fragilariopsis cylindrus* (CCMP 1102) were maintained in exponential growth phase (0.5–3 million cells mL^{-1}) at 0°C under continuous light (50 $\mu E\ m^{-2}\ s^{-1}$ supplied by GE Plant & Aquarium fluorescents). Cells were grown in sterile 2-L teflon bottles in double-filtered (0.2 μm) Antarctic Ross sea water amended with double L1 + Si nutrient mix (Guillard and Hargraves, 1993) and bubbled with sterile air (140 mL min^{-1}) to ensure sufficient nutrient and CO_2 supplies. At time zero (T0) five biological replicate, high-density cultures (2–2.5 $\times$ 10^6 cells mL^{-1}) were divided into duplicate teflon vessels. Serial dilutions were made with either control 35 salinity media or hyperosmotic media amended with sea salts (Instant Ocean) to achieve a final salinity of 70. In experiment I, nine dilutions were made over a 23-h period (treatment bottles shifted approximately 4 salinity units per dilution); in experiment II, four dilutions were made over a 22-h period (treatment bottles shifted approximately 8.5 salinity units per dilution). Cultures were sampled at T0 (before first dilution), T1 (24 h following first dilution), T2 (48 h), and T7 (168 h).

Abiotic Measurements

Culture irradiance values were measured by a quantum light meter (Biospherical Instruments, QSL-100) outfitted with a 4π submersible sensor. Salinity measurements were made with a hand-held optical refractometer with automatic temperature compensation (Vista Series Instruments). Osmolality was determined by a vapor pressure osmometer (Wescor, Vapro 5520). Culture pH was measured in 0.45-μM filtered subsamples kept on ice at experimental temperatures (Orion, Benchtop pHuture solid state pH system). For experiment I, carbonate alkalinity was determined based on pH change following a standard acid titration (Parsons et al., 1984); for experiment II it was determined using a spectrometric method (Sarazin et al., 1999).

Standard Cell Culture Measurements

Cell counts and biovolume were measured on technical duplicates using a Beckman-Coulter multisizer 3. Fluorometric quantification (Turner Designs, TD-700 fluorometer) of chlorophyll *a* was performed on subsamples filtered onto Whatman GF/F filters and extracted in 90% acetone for 24 to 48 h in the dark at 4°C. Absence of bacterial contamination was confirmed by epifluorescence microscopy of paraformaldehyde fixed subsamples stained with 4′,6-

diamidino-2-phenylindole and filtered onto 0.2-μm black polycarbonate filters (Sherr et al., 2001). 4′,6-Diamidino-2-phenylindole staining time was increased to overnight for optimal differentiation between *F. cylindrus* and bacteria cells.

DMSP Quantification

Samples were acidified with 50% H_2SO_4 for the determination of total DMSP and dissolved DMSP. Dissolved fractions were collected by gravity filtration through Whatman GF/F filters to remove cell particles. DMSP was quantified as DMS following NaOH base hydrolysis (1:1 M reaction) collected in a cryogenic purge and trap system coupled to a gas chromatograph, photometric flame detector unit (Hewlett-Packard 5890 series II). $DMSP_p$ was calculated from the difference between total and dissolved fractions (Kiene and Slezak, 2006). Intracellular DMSP was calculated by dividing $DMSP_p$ per mL by cell biovolume per mL to determine cellular DMSP molar concentrations.

F_v/F_m

F_v/F_m was measured by fast repetition rate fluorometry using a FastTracka instrument (Chelsea Instruments). Culture aliquots were dark adapted on ice prior to F_v/F_m readings. Optimal dark adaptation time for *F. cylindrus* was determined to be 15 to 35 min based on preliminary optimization experiments (data not shown). To avoid temperature stress the cell chamber was chilled externally with ice and internally with cold sea water. Chilled control and treatment salinity seawater was used to dilute cells in the chamber to produce readings within the optimal instrument sensitivity range. F_v/F_m was calculated from the average of five acquisitions.

Biomass Collection and Extraction

Cells were collected at T2 for proteomics and qPCR and T7 for qPCR by centrifugation of a total of 800 mL of culture per biological replicate. Two aliquots of 400-mL culture were spun in 500-mL vessels at 2,000*g*, 0°C for 10 min. The majority of the supernatant was poured off, cells were resuspended in approximately 20 mL, equal volumes were divided into two 15-mL vials, and recentrifuged for 2 min at 2,000*g*. Again a majority of supernatant was removed and approximately 3 mL of resuspended cells was equally divided into 2-mL eppendorf tubes. A final spin was performed for 2 min. Supernatant was aspirated off, pellets were flash frozen, and stored at −80°C.

Protein and RNA were extracted from frozen cell pellets using TRIzol reagent (Invitrogen Molecular Probes). The following modifications were made to the manufacturer's directions to optimize retrieval from sea-ice diatom cells. Cells were lysed in Trizol by repetitive pipetting (0.8 mL per 1–4 × 10^8 cells) and incubated at room temperature for approximately 15 min. The top layer containing RNA was added to isoproponal and stored at −20°C. Precipitated protein was washed three times with 0.3-M guanidine hydrochloride in 95% ethanol. During wash steps pellets were sonicated using a tip sonicator set on low, two to three times for 3 s, chilling on ice between sonications. Protein pellets were dried under vacuum, then resuspended in rehydration buffer (7 M urea, 2 M thiourea, 30 mM Tris pH 8.5, 4% CHAPS). Proteins were solubilized for 24 to 48 h at 4°C, followed by low-speed vortex at room temperature for 30 to 60 min. Insoluble material was removed by 30-min ultracentrifugation (100,000*g*) at 15°C. The supernatant was transferred to a fresh tube and protein concentration was determined in triplicate using the Bradford method (Bradford, 1976) with protein assay dye reagent concentrate (Bio-Rad) and bovine serum albumin protein standards (Thermo Scientific).

2DE and Image Analysis of T2 Proteins

Equal amounts of protein (150 μg per sample) were brought up to a final volume of 300 μL rehydration buffer amended with 60 mM dithiothreitol (DTT), 0.2% biolytes pH 3 to 10 (Bio-Rad), and 280 units of benzonase (Sigma-Aldrich). Immobilized pH 4 to 7 gradient strips (17 cm, Bio-Rad) were rehydrated with the sample by passive overnight rehydration. Isoelectric focusing was performed in PROTEAN IEF cells (Bio-Rad) with a maximum current of 50 μA/strip. Strips were actively desalted at 50 V for 1.5 h, followed by linear increase to a maximum of 8,000 V over 1 h. Wicks were then changed and focusing was completed by increasing voltage linearly to 10,000 V for 1 h, followed by a rapid increase to 10,000 V for 55,000 V h. Focused strips were then frozen at −80°C.

Prior to second dimension separation, proteins were sequentially reduced and alkylated in equilibration buffer containing 6 M urea, 0.375 M Tris pH 8.8, 2% SDS, and 20% glycerol. For reducing, thawed strips were gently rocked for 30 min in equilibration buffer with 2.5% DTT. Reducing buffer was aspirated off and strips were then alkylated by gently rocking for another 30 min in the dark with equilibration buffer plus 3% iodoacetamide (IAA). Strips were loaded on 12% polyacrylamide gels approximately 1 cm to the right of a wick soaked in 10 μL of precision plus protein unstained standards (Bio-Rad) and overlaid with bromophenol blue tinted agarose. SDS-PAGE separation was performed in Protean II ζ cell system units maintained at 15°C. Gels were electrophoresed in 25 mM Tris, 190 mM Gly, 0.1% SDS running buffer at 6 mA for 10 min, 16 mA for 30 min, and 24 mA for approximately 4 h (per gel) until the bromophenol blue front was roughly 1 cm from bottom of gel. Gels were fixed with 10% methanol/7% acetic acid, then stained overnight with Sypro Ruby (Invitrogen), rinsed with water, destained with 10% methanol/7% acetic acid, washed with water, and imaged on an FX pro plus fluorescent imager (Bio-Rad).

Control and treatment pairs were always run together to evenly distribute any variability in gel running conditions. Two to three technical replicates were run per sample and the best gel selected for analysis using PDQuest software, version 7.1 (Bio-Rad). Spots were detected automatically and matched across the 10 sample gels. The matchset was manually edited in appropriate magnification and contrast settings to confirm and improve matches. Novel spots were added to master and other gels to enable comparison across gels. Relative spot intensity (cumulative pixel intensity) was normalized to total intensity of all valid spots on each gel. A quantity table for all spots on all gels was exported to a spreadsheet for statistical analysis using MATLAB (version 2010, Mathworks, Inc.). *P* values for log-normalized spot intensities were calculated using the mattest function to perform two-sample *t* tests with permutations. The mafdr function was then used to calculate *q* values that correct for FDR inherent in multiple comparisons within large transcriptomic and proteomic datasets (Storey, 2002).

Digestion and Tandem Mass Spectrometry

Spots with *P* values ≤ 0.02 based on Student's *t* test and with intensities deemed high enough to enable mass spectrometry identification were added to a pick list for robotic gel extraction. Four to six gel plugs were pooled from treatment and control gels into 0.5-mL polypropylene eppendorf tubes. The pH was adjusted with 100 mM ammonium bicarbonate (NH_4HCO_3). Plugs were then destained through a series of washes with 50% acetonitrile (ACN) 50% NH_4HCO_3, and then dehydrated in 100% ACN. ACN was removed and plugs were air dried prior to reduction in 10 mM DTT in 100 mM NH_4HCO_3 for 45 to 60 min at 56°C. DTT was removed after cooling to room temperature, and proteins were alkylated in 55 mM IAA in 100 mM NH_4HCO_3 for 45 min in the dark. IAA was removed, pH again adjusted with 100 mM NH_4HCO_3 followed by 50% ACN 50% NH_4HCO_3 washes, dehydration with 100% ACN, and air drying of plugs. Trypsin gold (Promega) was reconstituted in 50 mM acetic acid to make a stock solution of 1 $\mu g \mu L^{-1}$ and aliquots stored at −80°C. Immediately prior to digestion, stock solution was brought up to a concentration of 25 $\mu g mL^{-1}$ of trypsin in 10% ACN 40 mM NH_4HCO_3 and 20 μL added to each tube of pooled plugs. Protein plugs were digested at 37°C overnight. Digestion was stopped by cooling to room temperature. Digest solution was transferred to clean 0.5-mL tubes. Remaining peptides were removed from plugs by vortexing and sonicating in 50% ACN 2% formic acid and this supernatant was added to digest solution. Peptides were dried down in a speed vac at low setting and stored at −20°C.

First attempts at protein spot identifications were performed by MALDI mass spectrometry. Peptide samples were reconstituted in 10 μL 0.1% trifluoroacetic acid by vortexing and sonication. Samples were purified and concentrated with a C18 Ziptip (Millipore) according to manufacturer's instructions. Peptides were eluted directly onto the MALDI target in 2 μL α-cyano-4-hydroxycinnamic acid matrix (10 $mg mL^{-1}$ in 50% ACN 50% 0.1% trifluoroacetic acid). Samples were processed on an Applied Biosystems 4800 proteomics analyzer externally calibrated according to manufacturer's protocol. Sample peptide masses in the mass-to-charge ratio range of 800 to 3,500 were collected in positive reflectron mode with a delayed extraction time and 2,000 laser shots per spectrum. The 12 most abundant peaks were selected as precursors for MS/MS analysis in a subsequent batch run.

Protein spots unable to be identified by MALDI data were recollected from additional control and treatment gels for analysis using LTQ. Dried peptides were resuspended in 20 μL of mobile phase A, vortexed, and sonicated. Any insoluble particles were removed by centrifugation (20,000*g*, 4°C, 10 min)

prior to transferring the sample solution to autosample vials. Buffers for the nano LC system (LC Packings) were made from HPLC grade reagents (mobile phase A: 98% water, 2% ACN, 0.2% formic acid, mobile phase B: 95% ACN, 5% water, 0.2% formic acid). An autosampler injected 15 μL of sample onto a 30-cm 75-μm C-18 reversed-phase LC column packed with YMC ODS-AQ resin (Waters Corp.). Peptides were eluted over a linear 60-min gradient from 4% B to 60% B. The column interfaced with a XCalibur LTQ (Thermo Finnigan) set to data-dependent analysis with collision-induced dissociation. Primary scans covered a mass-to-charge ratio range of 400 to 2,000. Secondary scans were performed on the five most abundant precursors with a minimum signal threshold of 1,000 and 3-min dynamic exclusion of precursor ions selected twice within a 30-s period.

Database Searching

MS/MS data were searched against *F. cylindrus* v1 genome filtered models 1 and all models FASTA databases downloaded from the U.S. Department of Energy Joint Genome Institute (JGI; http://genome.jgi-psf.org/Fracy1/Fracy1.home.html). The filtered models database includes only the best gene model per locus, while the all models database includes alternative gene models. Random decoy databases were generated for both filtered and all models to set thresholds for protein identification. Primary and secondary MALDI spectrum data were exported into GPS explorer (V3.6, Applied Biosystems) interfaced with the MASCOT (V2.1, Matrix Science) server to process spectrum and identify protein matches using MASCOT algorithm searches of *F. cylindrus* databases. Search parameters were set for trypsin digest with up to two missed cleavages, variable modifications of carbamidomethyl (Cys) and/or oxidation (Met), a peptide tolerance of 1 D, and MS/MS tolerance of 0.5 D. LTQ spectrum data were processed using Bioworks (Rev. 3.3.1 SP1, Thermo Finnigan) and SEQUEST search algorithm of *F. cylindrus* databases indexed for trypsin digestion with up to two missed cleavages, carbamidomethyl (Cys) and/or oxidation (Met) variable modifications, a peptide tolerance of 2 D, and MS/MS tolerance of 1 D. Protein scores that exceeded scores that were generated by the decoy database were considered candidate true identifications. Candidate true protein identifications were submitted to a second round of selection using scoring tools in SCAFFOLD (v3.00.08, Proteome Software, Inc.). MASCOT and SEQUEST files were uploaded and peptides additionally scored with a built-in search engine, X! Tandem (version 2007.01.01.1, The Global Proteome Machine Organization, http://thegpm.org). Peptide identifications were accepted if they could be established at >95% probability as specified by the peptide prophet algorithm (Keller et al., 2002). Protein identifications were accepted if they could be established at >95% probability and contained at least one identified peptide for MALDI samples and two peptides for LTQ. Protein probabilities were assigned by the protein prophet algorithm (Nesvizhskii et al., 2003). Proteins that contained similar peptides and could not be differentiated based on MS/MS analysis alone were grouped to satisfy the principles of parsimony.

If multiple significant hits were identified within a spot, protein identification was assigned to the best protein match (highest score, most peptides, and best-matching MW and pI). If a top hit could not be established because the spot was a mix of proteins that appear to be equally abundant based on spectrum counts then multiple identifications were listed. Protein spots 8,407 and 4,514 were analyzed on the MALDI with MASCOT search engine, as well as the LTQ with SEQUEST search algorithm to confirm LTQ best-match assignment methods agreed with MALDI identifications. Protein names reported are those assigned in the *F. cylindrus* genome based on best hit descriptions and KOG assignments through JGI automated annotation or by independent National Center for Biotechnology Information blastp searches of nonredundant protein sequences. Identifications based on the latter are specially noted and search results are listed in Supplemental Table S7.

Real-Time qPCR

Genes for five significantly changing proteins of interest and one housekeeping gene were selected for evaluation at the transcriptional level. Primers were designed manually then assessed for optimal Tm, hairpins, and dimer issues using online tools (http://www.idtdna.com/analyzer/Applications/OligoAnalyzer/; Integrated DNA Technology). Primer sequences (HPLC purified custom primers, Sigma-Aldrich) are listed in Supplemental Table S8. The RNA fraction from the Trizol protein isolation was precipitated with isopropanol and centrifuged at 12,000*g* for 8 min at 4°C. Pellets were washed with 75% ethanol, dried thoroughly, and resuspended in RNase-free water with Rnasein RNase inhibitor (Promega). Contaminating DNA was removed by DNase I digestion in solution and RNA was further purified using RNeasy MiniElute cleanup kits (Qiagen). RNA concentrations, 260/280, and 260/230 absorbance ratios were quantified in duplicate readings on the NanoDrop 2000 (Thermo Scientific). RNA quality was verified on a RNA 6000 Nano chip with a Bioanalyzer 2100 (Agilent). First-strand synthesis was performed using Superscript III reverse transcriptase (Invitrogen). Duplicate 50-μL reverse transcription reactions using random hexamers and 800-ng RNA were performed for each biological replicate. As a control to estimate DNA contamination, RNA was pooled from each biological replicate and first-strand synthesis components were added omitting reverse transcriptase to confirm the absence of genomic DNA. SYBR green PCR master mix (ABI) was used for second-strand amplification. Five to seven point standard curves were made from 1:2 serial dilutions of pooled reverse transcriptions. Amplifications were performed in 96-well plates on a 7500 real-time PCR system (ABI) using the following conditions: 10 min, 95°C denaturation step, followed by 40 amplification and quantification cycles of 15 s at 95°C, 40 s at 56°C to 64°C (see Supplemental Table S8 for primer sequences, optimized annealing temperatures, and concentrations), 40 s at 72°C, followed by melting curve analysis. Cycle threshold was automatically determined to provide the lowest SD in technical replicates fractional cycle number (CT) when fluorescence passes the threshold. Quadruplicate 20-μL reactions containing 2 μL of standard or diluted sample (1:10) were performed. Primer concentration and reaction temperature was optimized to produce single-peak melt curves and achieve reaction efficiencies between 90% and 110%. Efficiencies were incorporated into relative transcript abundance calculations according to Pfaffl (2001). Transcript abundance ratios were normalized to a reference housekeeping gene (18s RNA). Differences in normalized RNA abundance was determined using the REST-2009 program (Qiagen) that uses Bayesian randomization techniques to determine a posterior probability distributions to calculate *P* values of observed expression differences between treatment and controls occurring by chance (Pfaffl et al., 2002).

Protein Presequence Signal Analysis

Potential DMSP pathway genes identified from 2DE gels were screened for subcellular localization presequences (Emanuelsson et al., 2007). Because the N-terminal region is often poorly predicted, alternative N-terminal extensions, along with blast protein matches from the other two sequenced diatoms, *Thalassiosira pseudonana* (http://genome.jgi-psf.org/Thaps3/Thaps3.home.html) and *Phaeodactylum tricornutum* (http://genome.jgi-psf.org/Phatr2/Phatr2.home.html) were also screened for the presence of chloroplast bipartite targeting signals. Signal peptides and cleavage site predictions were performed by SignalP 3.0 (http://www.cbs.dtu.dk/services/SignalP/) and manually evaluated for the conserved diatom chloroplast motif ASAFAP at the signal peptide cleavage site (Gruber et al., 2007). Plastid transit peptide domains were identified by TargetP (http://www.cbs.dtu.dk/services/TargetP/). Proteins were classified as plastid targeted according to the methods of Kroth and colleagues (2008) if they (1) possess a signal peptide and no endoplasmic reticulum retention signal, (2) possess some transit peptide features beyond the N-terminal signal peptide and prior to the start of the conserved domain of the mature protein, and (3) contain one of the bulky hydrophobic amino acids (Phe, Trp, Tyr, or Leu) in the +1 position of the signal peptide cleavage site.

Statistical Analysis

Growth, F_v/F_m, and DMSP data were analyzed using the open source statistical software R (R Development Core Team, 2010). Raw data and residuals were graphed and assessed visually and mathematically for normality and homoscedasticity. The data were best explained using a general linear mixed effects model with biological replicates accounting for a random effect and treatment and time points as fixed effects. As would be expected, treatment and time showed individual as well as interactive effects on various parameters examined. Therefore, treatment effect *P* values were calculated for individual time points using Tukey's post-hoc analysis. Statistics for protein and gene expression data are explained in their respective method subsections above.

Sequence data from this article can be found in the Department of Energy JGI *F. cylindrus* genome library under the accession numbers listed in this article.

Supplemental Data

The following materials are available in the online version of this article.

Supplemental Table S1. Abiotic variables associated with salinity change.

Supplemental Table S2. Quantification table of T2 2DE gels.

Supplemental Table S3. Mass spectrometry identification scores for hypersalinity response proteins in *F. cylindrus*.

Supplemental Table S4. Complete LTQ-SEQUEST results.

Supplemental Table S5. Transcript abundance changes at high salinity relative to control.

Supplemental Table S6. Subcellular localization predictions from protein signal peptides.

Supplemental Table S7. Blast and KOG search results for unknown *F. cylindrus* proteins.

Supplemental Table S8. qPCR primer sets.

ACKNOWLEDGMENTS

We thank Tyler Cyronak and Amanda McLenon for help with experimental sampling and Alison Bland, Elizabeth Favre, and Dr. Benjamin Neely for proteomic technical and analytical support. Jennifer Bethard provided assistance at the Medical University of South Carolina Proteomics Core. We appreciate the assistance of Dr. Thomas Mock for early access to the *F. cylindrus* genome and assistance with chloroplast signal peptide prediction. Dr. John Schwacke provided the shuffled decoy FASTA databases and Dr. Allan Strand assisted with statistical analysis utilizing R. *F. cylindrus* sequence data were produced by the U.S. Department of Energy JGI (http://www.jgi.doe.gov/) in collaboration with the user community. This article is contribution number GMBL 379 of the Grice Marine Laboratory (College of Charleston).

Received August 9, 2011; accepted October 24, 2011; published October 27, 2011.

LITERATURE CITED

Allakhverdiev SI, Nishiyama Y, Suzuki I, Tasaka Y, Murata N (1999) Genetic engineering of the unsaturation of fatty acids in membrane lipids alters the tolerance of Synechocystis to salt stress. Proc Natl Acad Sci USA **96:** 5862–5867

Allen AE, Laroche J, Maheswari U, Lommer M, Schauer N, Lopez PJ, Finazzi G, Fernie AR, Bowler C (2008) Whole-cell response of the pennate diatom Phaeodactylum tricornutum to iron starvation. Proc Natl Acad Sci USA **105:** 10438–10443

Beligni MV, Yamaguchi K, Mayfield SP (2004) Chloroplast elongation factor ts pro-protein is an evolutionarily conserved fusion with the s1 domain-containing plastid-specific ribosomal protein-7. Plant Cell **16:** 3357–3369

Bradford MM (1976) A rapid and sensitive method for the quantitation of microgram quantities of protein utilizing the principle of protein-dye binding. Anal Biochem **72:** 248–254

Charlson RJ, Lovelock JE, Andreae MO, Warren SG (1987) Oceanic phytoplankton, atmospheric sulphur, cloud albedo and climate. Nature **326:** 655–661

Cock JM, Sterck L, Rouzé P, Scornet D, Allen AE, Amoutzias G, Anthouard V, Artiguenave F, Aury JM, Badger JH, et al (2010) The Ectocarpus genome and the independent evolution of multicellularity in brown algae. Nature **465:** 617–621

Cybis J, Davis RH (1975) Organization and control in the arginine biosynthetic pathway of Neurospora. J Bacteriol **123:** 196–202

Davison IR, Reed RH (1985) The physiological significance of mannitol accumulation in brown algae: the role of mannitol as a compatible cytoplasmic solute. Phycologia **24:** 449–457

DiTullio GR, Garrison DL, Mathot S (1998) Dimethylsulfonioproprionate in sea ice algae from the Ross Sea polynya. *In* KR Arrigo, MP Lizotte, eds, Antarctic Sea Ice: Biological Processes, Interactions and Variability. American Geophysical Union, Washington DC, pp 139–146

Dougan DA, Reid BG, Horwich AL, Bukau B (2002) ClpS, a substrate modulator of the ClpAP machine. Mol Cell **9:** 673–683

Edwards R, Dixon DP, Walbot V (2000) Plant glutathione S-transferases: enzymes with multiple functions in sickness and in health. Trends Plant Sci **5:** 193–198

Emanuelsson O, Brunak S, von Heijne G, Nielsen H (2007) Locating proteins in the cell using TargetP, SignalP and related tools. Nat Protoc **2:** 953–971

Feng Y, Xue Q (2006) The serine carboxypeptidase like gene family of rice (Oryza sativa L. ssp. japonica). Funct Integr Genomics **6:** 14–24

Friedman AL, Alberte RS (1986) Biogenesis and light regulation of the major light harvesting chlorophyll-protein of diatoms. Plant Physiol **80:** 43–51

Gage DA, Rhodes D, Nolte KD, Hicks WA, Leustek T, Cooper AJ, Hanson AD (1997) A new route for synthesis of dimethylsulphoniopropionate in marine algae. Nature **387:** 891–894

Gao Z, Loescher WH (2000) NADPH supply and mannitol biosynthesis: characterization, cloning, and regulation of the non-reversible glyceraldehyde-3-phosphate dehydrogenase in celery leaves. Plant Physiol **124:** 321–330

Göthel SF, Marahiel MA (1999) Peptidyl-prolyl cis-trans isomerases, a superfamily of ubiquitous folding catalysts. Cell Mol Life Sci **55:** 423–436

Greenbaum D, Colangelo C, Williams K, Gerstein M (2003) Comparing protein abundance and mRNA expression levels on a genomic scale. Genome Biol **4:** 117

Gröne T, Kirst GO (1992) The effect of nitrogen deficiency, methionine and inhibitors of methionine metabolism on the DMSP contents of *Tetraselmis subcordiformis* (Stein). Mar Biol **112:** 497–503

Gruber A, Vugrinec S, Hempel F, Gould SB, Maier UG, Kroth PG (2007) Protein targeting into complex diatom plastids: functional characterisation of a specific targeting motif. Plant Mol Biol **64:** 519–530

Guillard RRL, Hargraves PE (1993) *Stichochrysis immobilis* is a diatom, not a chyrsophyte. Phycologia **32:** 234–236

Hefu Y, Kirst GO (1997) Effect of UV-radiation on DMSP content and DMS formation of *Phaeocystis antarctica*. Polar Biol **18:** 402–409

Ito T, Asano Y, Tanaka Y, Takabe T (2011) Regulation of biosynthesis of dimethylsulfoniopropionate and its uptake in sterile mutant of *Ulva pertusa* (chlorophyta). J Phycol **47:** 517–523

Janech MG, Krell A, Mock T, Kang JS, Raymond JA (2006) Ice-binding proteins from sea ice diatoms (Bacillariophyceae). J Phycol **42:** 410–416

Janknegt PJ, Van De Poll WH, Visser RJW, Rijstenbil JW, Buma AGJ (2008) Oxidative stress responses in the marine antarctic diatom Chaetoceros brevis (bacillariophyceae) during photoacclimation. J Phycol **44:** 957–966

Karsten U, Wiencke C, Kirst GO (1990) The effect of light intensity and daylength on the beta-dimethylsulphoniopropionate (DMSP) content of marine green macroalgae from Antarctica. Plant Cell Environ **13:** 989–993

Karsten U, Wiencke C, Kirst GO (1992) Dimethylsulphonio-propionate (DMSP) accumulation in green macroalgae from polar to temperate regions: interactive effects of light versus salinity and light versus temperature. Polar Biol **12:** 603–607

Katsuhara M, Otsuka T, Ezaki B (2005) Salt stress-induced lipid peroxidation is reduced by glutathione S-transferase, but this reduction of lipid peroxides is not enough for a recovery of root growth in Arabidopsis. Plant Sci **169:** 369–373

Keller A, Nesvizhskii AI, Kolker E, Aebersold R (2002) Empirical statistical model to estimate the accuracy of peptide identifications made by MS/MS and database search. Anal Chem **74:** 5383–5392

Keller MD, Bellows WK, Guillard RRL (1989) Dimethyl sulfide production in marine phytoplankton. *In* ES Saltzman, WJ Cooper, eds, Biogenic Sulfur in the Environment. American Chemical Society, Washington, DC, pp 131–142

Kiene RP, Slezak D (2006) Low dissolved DMSP concentrations in seawater revealed by small-volume gravity filtration and dialysis sampling. Limnol Oceanogr Methods **4:** 80–95

Kirch H-H, Bartels D, Wei Y, Schnable PS, Wood AJ (2004) The ALDH gene superfamily of Arabidopsis. Trends Plant Sci **9:** 371–377

Kirst GO (1990) Salinity tolerance of eukaryotic marine algae. Annu Rev Plant Physiol Plant Mol Biol **41:** 21–53

Kirst GO, Thiel C, Wolff H, Nothnagel J, Wanzek M, Ulmke R (1991) Dimethylsulfoniopropionate (DMSP) in ice-algae and its possible biological role. Mar Chem **35:** 381–388

Kitaguchi H, Uchida A, Ishida Y (1999) Purification and characterization of L-methionine decarboxylase from Crypthecodinium cohnii. Fish Sci **65:** 613–617

Klatt P, Lamas S (2000) Regulation of protein function by S-glutathiolation in response to oxidative and nitrosative stress. Eur J Biochem **267:** 4928–4944

Koca H, Bor M, Özdemir F, Türkan I (2007) The effect of salt stress on lipid peroxidation, antioxidative enzymes and proline content of sesame cultivars. Environ Exp Bot **60:** 344–351

Krell A (2006) Salt Stress Tolerance in the Psychrophilic Diatom *Fragilariopsis cylindrus*. University of Bremen, Germany

Krell A, Funck D, Plettner I, John U, Dieckmann G (2007) Regulation of proline metabolism under salt stress in the psychrophilic diatom *Fragilariopsis cylindrus* (Bacillariophyceae). J Phycol **43:** 753–762

Krembs C, Deming JW (2008) The role of exopolymers in microbial adaptation to sea ice. *In* R Margesin, F Schinner, J-C Marx, C Gerday, eds, Psychrophiles: From Biodiversity to Biotechnology. Springer, Berlin, pp 247–264

Krembs C, Eicken H, Deming JW (2011) Exopolymer alteration of physical properties of sea ice and implications for ice habitability and biogeochemistry in a warmer Arctic. Proc Natl Acad Sci USA **108:** 3653–3658

Krembs C, Eicken H, Junge K, Deming JW (2002) High concentrations of exopolymeric substances in Arctic winter sea ice: implications for the polar ocean carbon cycle and cryoprotection of diatoms. Deep Sea Res Oceanogr Res Paper **49:** 2163–2181

Kroth PG, Chiovitti A, Gruber A, Martin-Jezequel V, Mock T, Parker MS, Stanley MS, Kaplan A, Caron L, Weber T, et al (2008) A model for carbohydrate metabolism in the diatom Phaeodactylum tricornutum deduced from comparative whole genome analysis. PLoS ONE **3:** e1426

Kumar S, Dhingra A, Daniell H (2004) Plastid-expressed betaine aldehyde dehydrogenase gene in carrot cultured cells, roots, and leaves confers enhanced salt tolerance. Plant Physiol **136:** 2843–2854

Lee PA, De Mora SJ, Gosselin M, Levasseur M, Bouillon R, Nozais C, Michel C (2001) Particulate dimethylsulfoxide in Arctic sea-ice algal communities: the cryoprotectant hypothesis revisited. J Phycol **37:** 488–499

Levasseur M (1994) A new source of dimethylsulfide (DMS) for the Arctic atmosphere: ice diatoms. Mar Biol **121:** 381–387

Lima A, Lima S, Wong JH, Phillips RS, Buchanan BB, Luan S (2006) A redox-active FKBP-type immunophilin functions in accumulation of the photosystem II supercomplex in Arabidopsis thaliana. Proc Natl Acad Sci USA **103:** 12631–12636

Mahfouz MM, Kummerow FA (2004) Vitamin C or vitamin B6 supplementation prevent the oxidative stress and decrease of prostacyclin generation in homocysteinemic rats. Int J Biochem Cell Biol **36:** 1919–1932

McCarthy AA, McCarthy JG (2007) The structure of two N-methyltransferases from the caffeine biosynthetic pathway. Plant Physiol **144:** 879–889

Mock T, Krell A, Glockner G, Kolukisaoglu U, Valentin K (2005) Analysis of expressed sequence tags (ESTs) from the polar diatom *Fragilariopsis cylindrus.* J Phycol **42:** 78–85

Mock T, Kroon BMA (2002a) Photosynthetic energy conversion under extreme conditions—I: important role of lipids as structural modulators and energy sink under N-limited growth in Antarctic sea ice diatoms. Phytochemistry **61:** 41–51

Mock T, Kroon BMA (2002b) Photosynthetic energy conversion under extreme conditions—II: the significance of lipids under light limited growth in Antarctic sea ice diatoms. Phytochemistry **61:** 53–60

Morgan-Kiss RM, Priscu JC, Pocock T, Gudynaite-Savitch L, Huner NP (2006) Adaptation and acclimation of photosynthetic microorganisms to permanently cold environments. Microbiol Mol Biol Rev **70:** 222–252

Mostaert AS, Karsten U, King RJ (1995) Physiological responses of Caloglossa leprieurii (Ceramiales, Rhodophyta) to salinity stress. Phycological Res **43:** 215–222

Mostaert AS, Orlovich DA, King RJ (1996) Ion compartmentation in the red alga Caloglossa leprieurii in response to salinity changes: freeze-substitution and x-ray microanalysis. New Phytol **132:** 513–519

Nesvizhskii AI, Keller A, Kolker E, Aebersold R (2003) A statistical model for identifying proteins by tandem mass spectrometry. Anal Chem **75:** 4646–4658

Nishiguchi MK, Somero GN (1992) Temperature- and concentration-dependence of compatibility of the organic osmolyte beta-dimethylsulfoniopropionate. Cryobiology **29:** 118–124

Nyyssölä A, Reinikainen T, Leisola M (2001) Characterization of glycine sarcosine N-methyltransferase and sarcosine dimethylglycine N-methyltransferase. Appl Environ Microbiol **67:** 2044–2050

Pandhal J, Ow SY, Wright PC, Biggs CA (2009) Comparative proteomics study of salt tolerance between a nonsequenced extremely halotolerant cyanobacterium and its mildly halotolerant relative using in vivo metabolic labeling and in vitro isobaric labeling. J Proteome Res **8:** 818–828

Papadimitriou S, Thomas DN, Kennedy H, Haas C, Kuosa H, Krell A, Dieckmann GS (2007) Biogeochemical composition of natural sea ice brines from the Weddell Sea during early austral summer. Limnol Oceanogr **52:** 1809–1823

Parsons TR, Maita Y, Lalli CM (1984) A Manual of Chemical and Biological Methods for Seawater Analysis. Pergammon Press, Oxford

Pfaffl MW (2001) A new mathematical model for relative quantification in real-time RT-PCR. Nucleic Acids Res **29:** e45

Pfaffl MW, Horgan GW, Dempfle L (2002) Relative expression software tool (REST) for group-wise comparison and statistical analysis of relative expression results in real-time PCR. Nucleic Acids Res **30:** e36

Premvardhan L, Bordes L, Beer A, Büchel C, Robert B (2009) Carotenoid structures and environments in trimeric and oligomeric fucoxanthin chlorophyll a/c2 proteins from resonance Raman spectroscopy. J Phys Chem B **113:** 12565–12574

Pulla R, Kim Y-J, Parvin S, Shim J-S, Lee J-H, Kim Y-J, In J-G, Senthil K, Yang D-C (2009) Isolation of S-adenosyl-L-methionine synthetase gene from Panax ginseng C.A. meyer and analysis of its response to abiotic stresses. Physiol Mol Biol Plants **15:** 267–275

R Development Core Team (2010) R: A Language and Environment for Statistical Computing. R Foundation for Statistical Computing, Vienna

Raymond JA (2011) Algal ice-binding proteins change the structure of sea ice. Proc Natl Acad Sci USA **108:** E198

Raymond JA, Janech MG, Fritsen CH (2009) Novel ice-binding proteins from a psychrophilic antarctic alga (chlamydomonadaceae, chlorophyceae). J Phycol **45:** 130–136

Rijstenbil JW (2005) UV- and salinity-induced oxidative effects in the marine diatom *Cylindrotheca closterium* during simulated emersion. Mar Biol **147:** 1063–1073

Rodriguez R, Redman R (2005) Balancing the generation and elimination of reactive oxygen species. Proc Natl Acad Sci USA **102:** 3175–3176

Ronimus RS, Morgan HW (2001) The biochemical properties and phylogenies of phosphofructokinases from extremophiles. Extremophiles **5:** 357–373

Sarazin G, Michard G, Prevot F (1999) A rapid and accurate spectroscopic method for alkalinity measurements in sea water samples. Water Res **33:** 290–294

Scala S, Carels N, Falciatore A, Chiusano ML, Bowler C (2002) Genome properties of the diatom *Phaeodactylum tricornutum*. Plant Physiol **129:** 993–1002

Sherr B, Sherr E, del Giorgio P (2001) Enumeration of total and highly active bacteria. *In* JH Paul, ed, Methods in Microbiology: Vol 30. Marine Microbiology. Academic Press, New York, pp 129–159

Slezak D, Herndl GJ (2003) Effects of ultraviolet and visible radiation on the cellular concentrations of dimethylsulfonio-propionate (DMSP) in *Emiliania huxleyi* (strain L). Mar Ecol Prog Ser **246:** 61–71

Srivastava AK, Bhargava P, Thapar R, Rai LC (2008) Salinity-induced physiological and proteomic changes in Anabaena doliolum. Environ Exp Bot **64:** 49–57

Stefels J (2000) Physiological aspects of the production and conversion of DMSP in marine algae and higher plants. J Sea Res **43:** 183–197

Storey J (2002) A direct approach to false discovery rates. J R Stat Soc Series B Stat Methodol **64:** 479–498

Sudhir P, Murthy SDS (2004) Effects of salt stress on basic processes of photosynthesis. Photosynthetica **42:** 481–486

Summers PS, Nolte KD, Cooper AJL, Borgeas H, Leustek T, Rhodes D, Hanson AD (1998) Identification and stereospecificity of the first three enzymes of 3-dimethylsulfoniopropionate biosynthesis in a chlorophyte alga. Plant Physiol **116:** 369–378

Sunda W, Kieber DJ, Kiene RP, Huntsman S (2002) An antioxidant function for DMSP and DMS in marine algae. Nature **418:** 317–320

Sunda WG, Hardison R, Kiene RP, Bucciarelli E, Harada H (2007) The effect of nitrogen limitation on cellular DMSP and DMS release in marine phytoplankton: climate feedback implications. Aquat Sci **69:** 341–351

Sunkar R, Bartels D, Kirch HH (2003) Overexpression of a stress-inducible aldehyde dehydrogenase gene from Arabidopsis thaliana in transgenic plants improves stress tolerance. Plant J **35:** 452–464

Thomas DN, Dieckmann GS (2002) Antarctic sea ice—a habitat for extremophiles. Science **295:** 641–644

Trevena AJ, Jones GB, Wright SW, van den Enden RL (2000) Profiles of DMSP, algal pigments, nutrients and salinity in pack ice from eastern Antarctica. J Sea Res **43:** 265–273

Trossat C, Rathinasabapathi B, Weretilnyk EA, Shen TL, Huang ZH, Gage DA, Hanson AD (1998) Salinity promotes accumulation of 3-dimethylsulfoniopropionate and its precursor S-methylmethionine in chloroplasts. Plant Physiol **116:** 165–171

Vairavamurthy A, Andreae MO, Iverson RL (1985) Biosynthesis of dimethylsulfide and dimethylpropiothetin by *Hymenomonas carterae* in relation to sulfur source and salinity variations. Limnol Oceanogr **30:** 59–70

Vernon DM, Bohnert HJ (1992) A novel methyl transferase induced by osmotic stress in the facultative halophyte Mesembryanthemum crystallinum. EMBO J **11:** 2077–2085

Waditee R, Bhuiyan MNH, Rai V, Aoki K, Tanaka Y, Hibino T, Suzuki S, Takano J, Jagendorf AT, Takabe T, et al (2005) Genes for direct methylation of glycine provide high levels of glycinebetaine and abiotic-stress tolerance in Synechococcus and Arabidopsis. Proc Natl Acad Sci USA **102:** 1318–1323

Wilson MA, St Amour CV, Collins JL, Ringe D, Petsko GA (2004) The 1.8-A resolution crystal structure of YDR533Cp from Saccharomyces cerevisiae: a member of the DJ-1/ThiJ/PfpI superfamily. Proc Natl Acad Sci USA **101:** 1531–1536

Yi X, Hargett SR, Liu H, Frankel LK, Bricker TM (2007) The PsbP protein is required for photosystem II complex assembly/stability and photoautotrophy in Arabidopsis thaliana. J Biol Chem **282:** 24833–24841

Zubieta C, Ross JR, Koscheski P, Yang Y, Pichersky E, Noel JP (2003) Structural basis for substrate recognition in the salicylic acid carboxyl methyltransferase family. Plant Cell **15:** 1704–1716